Inorganic Chemistry

pubs.acs.org/IC
Article

Mechanochemical Synthesis of a Sodium Anion Complex [Na^+(2,2,2-cryptand)Na^-] and Studies of Its Reactivity: Two-Electron and One-Electron Reductions

Nathan Davison, Jack M. Hemingway,* Corinne Wills,* Tomislav Stolar, Paul G. Waddell,* Casey M. Dixon, Luke Barron, James A. Dawson, and Erli Lu*

Cite This: *Inorg. Chem.* 2024, 63, 15247−15258

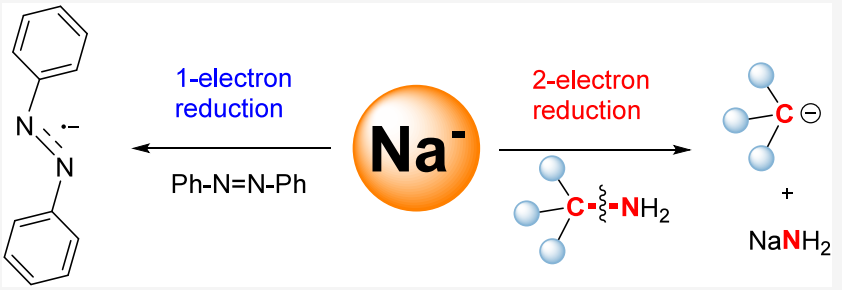

ABSTRACT: Group 1 metal molecular chemistry is dominated by a +1 oxidation state, while a 0 oxidation state is widespread in the metals. A more exotic, yet still available, oxidation state of group 1 metal is −1, i.e., alkalide. Reported as early as the 1970s, the alkalides appear in every modern inorganic chemistry textbook as an iconic chemical curiosity, yet their reactivity remains unexplored. This is due to their synthetic hurdles. In this work, we report the first facile synthesis of the archetypical alkalide complex, [Na^+(2,2,2-cryptand)Na^-], which allows us to unveil a versatile reactivity profile of this once exotic species.

INTRODUCTION

Reduction and oxidation (redox) reactions involve interconversions between an element's available oxidation states and are the cornerstones of organometallic catalysis, such as oxidative addition and reductive elimination. An element's redox chemistry is underpinned by its available oxidation states. For example, the Pd(0) ↔ Pd(+2) interconversion is the foundation of the classic Suzuki−Miyaura coupling.[1] Such single-metal two-electron redox processes are traditionally limited to transition metals, while recent efforts have expanded the scope to lanthanide,[2] actinide,[3,4] and p-block (groups 13−15[5]) (Figure 1) metals, as well as non-metal centers such as phosphorus.[6] From a sustainability perspective, developing main-group metal-mediated two-electron redox processes is crucially important for developing future sustainable catalysts and has hence attracted significant and fast-growing interest across the inorganic, organic, and catalysis communities.[5]

Group 1 alkali metals (AMs) are among the most abundant elements in the Earth's crust (e.g., Na has an abundance of 2.6%). There are three available oxidation states for the group 1 metals: +1, 0, and −1. While their molecular chemistry is exclusively in the +1 oxidation state, the one-electron AM(0) ↔ AM(+1) process plays essential roles in chemical synthesis as widely used reductants (e.g., potassium mirror and potassium graphite) as well as in batteries. Hitherto, single-metal two-electron processes, i.e., AM(−1) ↔ AM(+1), are unknown for the alkali metals, which is due to poor accessibility to an iconic chemical curiosity, the long-known yet surprisingly underdeveloped AM(−1) anions, i.e., the alkalides.

Since the first reports in the 1970s by the group of the late James Dye,[7−9] alkalides appear in every inorganic chemistry textbook.[10] Discussions about the nature of the exotic −1 oxidation-state alkali metal anions have continued until today,[11,12] along with several *in silico* theoretical studies from the physics and physical chemistry communities.[13−16] Nonetheless, from a synthetic chemistry perspective, the reactivity of alkalides, including their potential in two-electron redox chemistry, has never been properly studied apart from a few decomposition studies.[17,18] This *status quo* is due to their formidable synthetic hurdles.

The classical alkalide synthetic methods require technically demanding conditions, such as extremely volatile solvents (e.g.,

Received: July 12, 2024
Revised: July 20, 2024
Accepted: July 23, 2024
Published: July 29, 2024

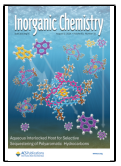

https://doi.org/10.1021/acs.inorgchem.4c02914
Inorg. Chem. 2024, 63, 15247−15258

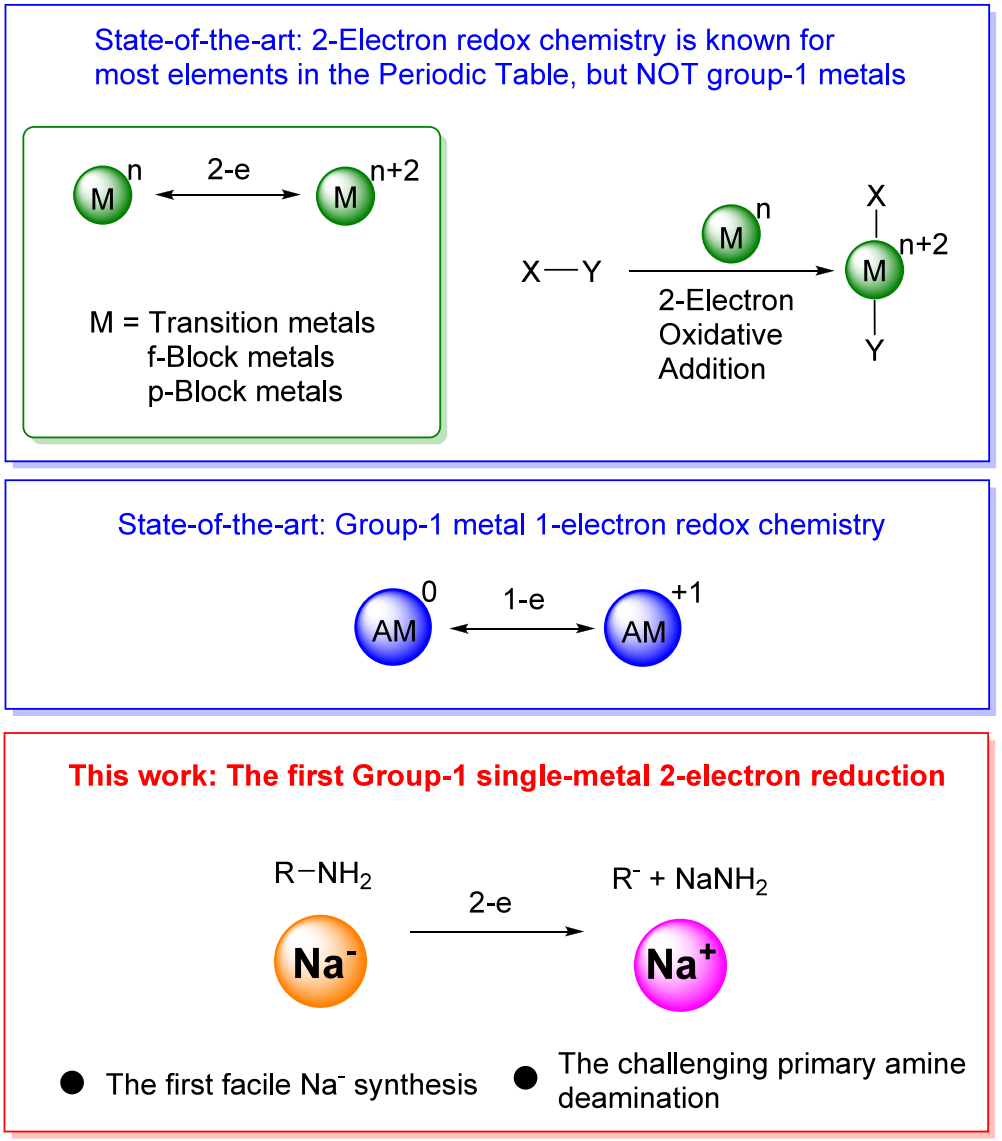

Figure 1. State of the art and this work. Two-electron redox chemistry is known for d-, p-, and f-block metals, but not for group 1 alkali metals (top). State-of-the-art group 1 metal redox chemistry (middle) and this work (bottom).

methylamine), specially designed glassware, and unconventional synthetic protocols (e.g., metal vapor deposition under 10^{-5} Torr high vacuum), and suffer from poor scalability and low yields.[19−23]

Herein, we overcome the alkalide synthetic hurdles by introducing a mechanochemical ball milling method.[24,25] The new protocol allows us to synthesize the archetypical alkalide, a sodide [Na^+(2,2,2-cryptand)Na^-] (**1**),[8] from readily available starting materials (sodium metal and 2,2,2-cryptand) at a millimole scale in reasonable and reproducible yield (≤48%). We characterize **1** as the modern standard and clarify several historical ambiguities and/or inaccuracies, especially with regard to ^{23}Na nuclear magnetic resonance (NMR) and single-crystal X-ray diffraction (SCXRD) studies, as well as its electronic structure via quantum chemical density functional theory (DFT) calculations. More importantly, we find that **1** exhibits a versatile reactivity profile, including the first alkali metal-mediated single-metal two-electron process (C−N cleavage deamination in primary amines), and also a one-electron reduction toward azobenzene. The findings are elaborated in the following sections.

RESULTS AND DISCUSSION

Inspired by recent success in the use of mechanochemical ball milling in s-block chemistry,[24,26−28] we tested a reaction between 2 equiv of sodium metal and 1 equiv of 2,2,2-cryptand. The ball milling reaction was first monitored in a 14 mL transparent poly(methyl methacrylate) (PMMA) jar under argon, at room temperature, at a frequency of 30 Hz. The starting materials were initially converted into a deep blue mixture within 1 min of milling and then into a golden substance within 10 min (Figure 2a). The fleet intermediate deep blue color indicates an interesting possibility: an electride intermediate was formed at the initial stage of milling, i.e., Na(0) + 2,2,2-cryptand → [Na^+(2,2,2-cryptand)e^-], which subsequently reduces Na(0) to Na^-, i.e., [Na^+(2,2,2-cryptand)-e^-] + Na(0) → [Na^+(2,2,2-cryptand)Na^-].

On the basis of visual observation, the preparative scale reaction condition was set as 30 Hz for 10 min at room

https://doi.org/10.1021/acs.inorgchem.4c02914
Inorg. Chem. 2024, 63, 15247−15258

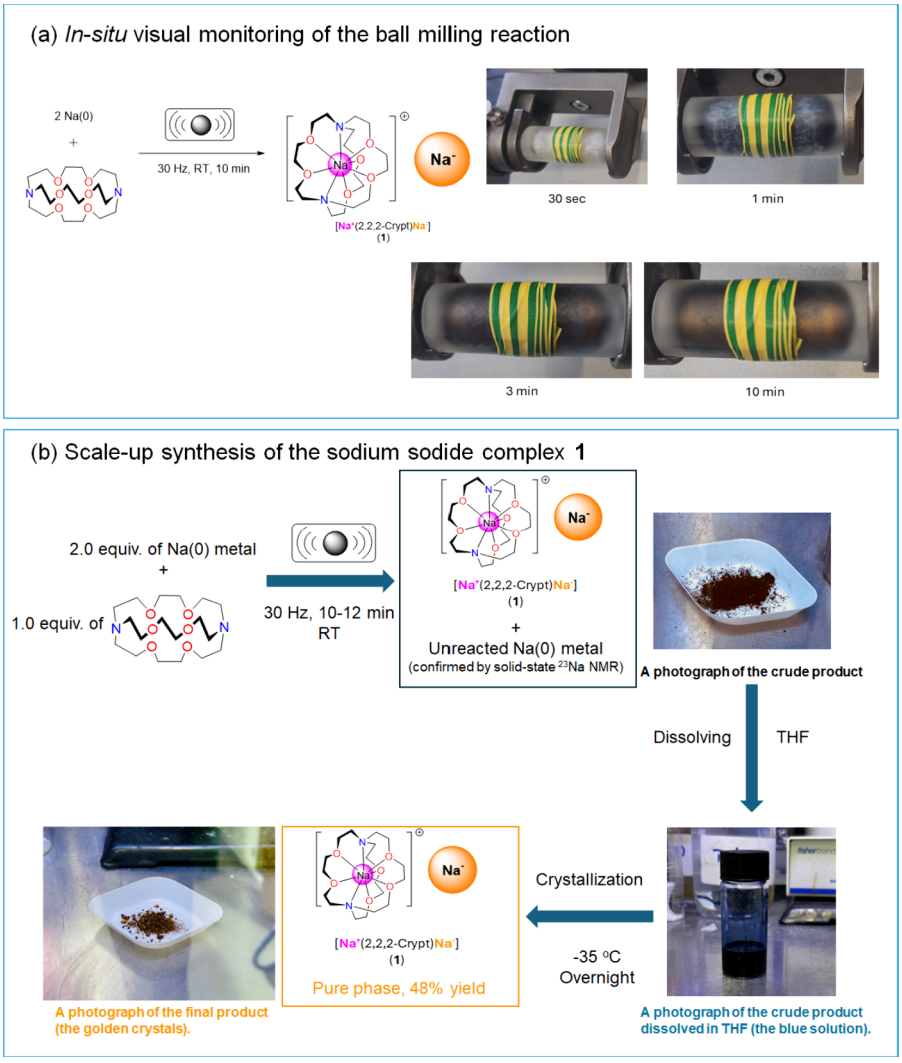

Figure 2. Mechanochemical synthesis of **1**. (a) *In situ* visual monitoring of the ball milling reaction between Na metal and 2,2,2-cryptand in a transparent PMMA jar. (b) Synthesis and crystallization of sodide complex **1**.

temperature. A black-brown solid crude product was produced (Figure 2b), which was proven to be a mixture of target sodide **1** and unreacted Na(0) metal by a magic angle spinning (MAS) solid-state ^{23}Na NMR spectrum (Figure 3 top). The two signals at −11 and −62 ppm represent Na^+ and Na^- of **1**, respectively. The chemical shifts of these two signals match Dye's reports in three solvents [tetrahydrofuran (THF), ethylamine, and methylamine][29] and those from a single-crystal ^{23}Na NMR study, as well.[30,31] The Na^- signal of **1** in Figure 3 also matches a recent report of a potassium sodide complex in solution by Barrett et al. (^{23}Na NMR chemical shifts −61 to −63 ppm),[32] despite crystalline material not being obtained therein. The Dye group and others conducted ^{23}Na NMR studies of **1** and other related sodides[33−35] and reported a sodium metal Na(0) contamination at 1120 ppm.[22c] The chemical shift matches the results of recent theoretical[36] and experimental[37] ^{23}Na NMR studies on the zerovalent metallic Na(0) species. Hence, we expanded our scanning range of the MAS ^{23}Na NMR for the crude product and indeed located a signal at 1134 ppm (Figure 3, top), which can be attributed to unreacted Na(0) metal, matching that which Gray and co-workers reported in their MAS ^{23}Na NMR studies in the Na-ion battery context.[36] Hence, we can conclude that the crude product from the ball milling is a mixture of **1**, unreacted Na(0) metal, and potentially unreacted 2,2,2-cryptand.

Pure **1** was obtained as golden/bronze crystals from a THF solution of the crude mixture after it had been kept at −35 °C overnight, and its SCXRD structure was again investigated. The crystals were found to be similar in appearance to those described by Dye et al. in their 1974 original report,[8] but our crystallization procedure is much simpler (THF left to stand in a −35 °C freezer vs slow evaporation and multiple washings with ethylamine at a cryogenic temperature). The bulk golden crystals were found to be thin flakes, as previously described in ref 9, and could be mounted on the goniometer of an X-ray diffractometer with little difficulty.

Whereas the structure of **1** in Dye's original report in 1974 (Cambridge Structural Database deposition reference CRYPNA10)[9] was determined with space group $R3_2$, we posit that the space group is more likely to be $I2$. The structure determined from the data reported here does solve in $R3_2$ but with much higher refinement metrics (e.g., R_1 = 6.80%, and wR_2 = 21.39%). Determining the structure in monoclinic space group $I2$ provides much better agreement with the data. Full crystallography details can be found in Table S1 (our new

https://doi.org/10.1021/acs.inorgchem.4c02914
Inorg. Chem. 2024, 63, 15247−15258

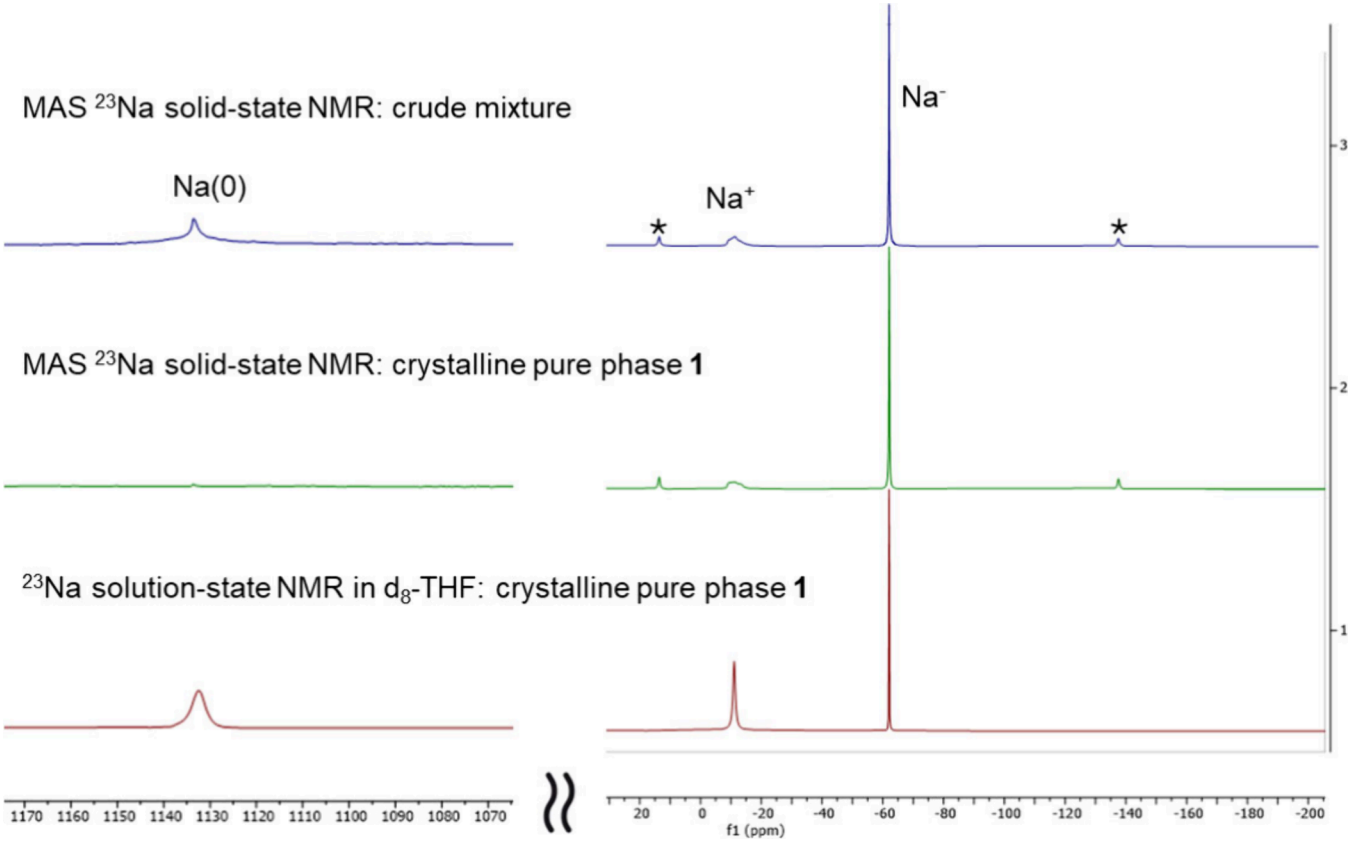

Figure 3. Solid-state and solution ^{23}Na NMR studies of **1** as the crude product and pure phase. Magic angle spinning (MAS) solid-state ^{23}Na NMR spectra of the crude mixture (top) and the pure phase of **1** (middle) and solution-state ^{23}Na NMR spectrum of the pure phase of **1** in d_8-THF (bottom). All of the NMR spectra were collected at 298 K. *MAS spinning sidebands.

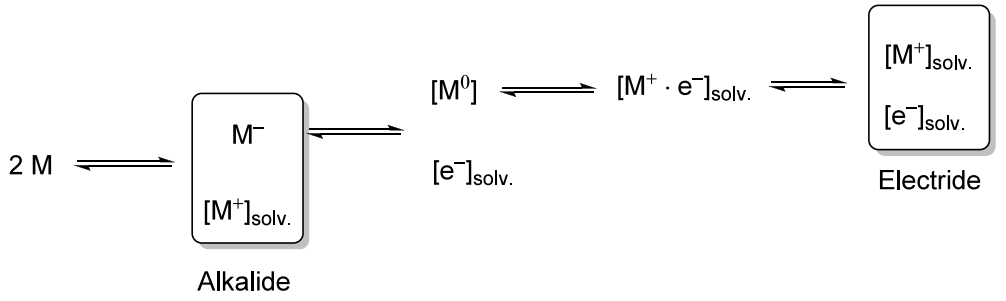

Figure 4. Equilibria between the alkalide and electride phases.

solution) and Table S2 (the previous solution), while the refined molecular structure of **1** can be found in Figure S22. The sodide anion, Na2, is found isolated from the rest of the structure. The Na$^-$—Na$^+$ distances from a sodide anion to its neighboring Na$^+$ cations are ∼7.0 Å. The anion—anion distances range from ∼8.7 to ∼10.9 Å, indicating that there are no anion—anion inter-alkalide interactions, which have been observed in some other sodides.[22c]

Once isolated, the golden crystals of **1** can be handled at room temperature for at least 12 h, allowing further characterization. The MAS ^{23}Na solid-state NMR study of the golden crystals confirmed that it is a pure phase of **1** (Figure 3, middle). While the −11 and −62 ppm signals persist, the 1134 ppm signal disappeared, indicating that the unreacted Na(0) metal was successfully removed. The crystalline yield of **1** was 48% at a 2 mmol scale (see Experimental Section at the end of the paper).

1 is insoluble in hexane and immediately reacts with benzene at room temperature, where the characteristic golden color disappears and an off-white suspension with intractable ^{1}H/^{23}Na NMR spectra is formed. Dissolving **1**'s crystals in d_8-THF resulted in a deep blue solution, which gave a surprising ^{23}Na NMR spectrum. The 1134 ppm signal of Na(0) reappears (Figure 3, bottom). The resurgence of the Na(0) signal in the THF solution may appear to be confusing, but it has been hypothesized for a long time that an alkalide can undergo a series of equilibria (Figure 4);[33e,f] this hypothesis was reported even before the discovery of the first crystalline alkalide **1**.[38] This equilibrium hypothesis was also supported by modern thermodynamic cycle calculations.[39] We hypothesize that such an equilibrium in the THF solution of **1** leads to the observed Na(0) signal.

Once isolated as the golden crystals, **1** is stable at room temperature under argon for at least 12 h, allowing the

https://doi.org/10.1021/acs.inorgchem.4c02914
Inorg. Chem. 2024, 63, 15247−15258

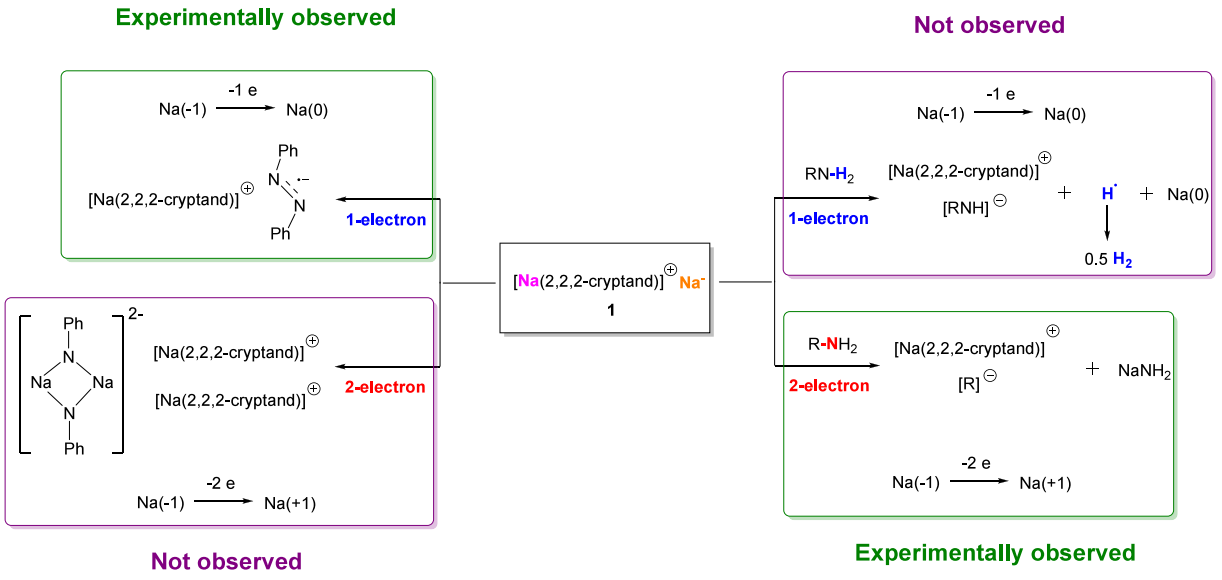

Figure 5. Possible one-electron and two-electron redox reaction pathways of **1**. Reactions between **1** and primary amines (right) or azobenzene (left) could take one-electron or two-electron pathways, but only one pathway is experimentally observed for each: the two-electron pathway for primary amines and the one-electron pathway for azobenzene.

following reactivity studies (*vide infra*). Storage at room temperature for a few days will eventually lead to decolorization of the golden crystals, which is a sign of decomposition. With regard to **1**'s thermal stability in a THF solution, we found that the rate of decolorization (decomposition) of the blue THF solution depends on the concentration. The more dilute the solution, the faster the decomposition, indicating the major decomposition pathway is reaction with the solvent THF, which corresponds well with the previous alkalide decomposition studies.[17,18] Whereas at a concentration of 0.25 mmol/L, the solution decolorized almost immediately (which prevented us from obtaining an ultraviolet−visible absorption spectrum), a NMR concentration (~0.1 mol/L in d_8-THF) solution was found to be stable at room temperature for ~2 h before eventually fading into a colorless solution (^{1}H NMR, only 2,2,2-cryptand; ^{23}Na NMR, only Na^+ species). We also conducted variable-temperature ^{23}Na NMR studies of **1** in d_8-THF in the temperature range of 243−313 K (Figures S7 and S8) and monitored the decomposition of **1** in d_8-THF (concentration of 80.5 mmol/L) at 313 K (Figures S9 and S10). The latter indicates that the Na(0) and Na^- signals disappear simultaneously upon decomposition, forming a Na^+ species with a broad ^{23}Na signal.

We conducted DFT calculations of **1**, which provide unprecedented insights into the electronic structure, especially the charge distribution and frontier molecular orbitals. A geometry optimization calculation well reproduced the SCXRD structure (see Section 2 of the Supporting Information for more detailed computational methods). On the basis of the optimized structure, we conducted natural bonding orbital (NBO) charge analysis, which is the most effective diagnostic parameter for distinguishing between a Na^+ and a Na^-. The NBO charge on Na^- was calculated as −0.880, in sharp contrast with the value of +0.823 on the Na^+. The NBO charges unquestionably confirm the sodide nature of **1**. We also calculated the isotropic NMR shielding tensors (in parts per million) of Na^+ and Na^-, which are 569.8745 and 629.8618 ppm, respectively. The relationship between the NMR shielding tensor ($\boldsymbol{\sigma}$) and the observed chemical shift (δ) is defined by Facelli[40] in the equation $\delta = a\sigma_{iso} - \boldsymbol{\sigma}$, where a is the unit matrix and σ_{iso} is the isotropic value or trace of the shielding tensor of a certain element's (here ^{23}Na) standard NMR reference. The difference between the calculated NMR shielding tensor of the Na^+ and Na^- centers in **1** agrees well with the experimentally observed chemical shift difference, as well as with the literature precedents.[31]

The improved access to **1** enabled by the ball milling method unlocks the gateway to test its reactivity. In principle, the Na^- center in **1** can conduct both one-electron [Na(−1) → Na(0)] and two-electron [Na(−1) → Na(+1)] reductions. We chose two classes of substrates to assess the one-electron versus two-electron reactivity: primary amines and azobenzene (Figure 5). Primary amines have two reactive sites: the N−H bond and the C−N bond. Among the two sites, the Brønsted acidic N−H bond is reactive, labile to Brønsted acid−base deprotonation and one-electron reductive deprotonation. The latter was very recently reported by the Harder group in a case of electride-mediated one-electron reductive deprotonation.[41] Along with the one-electron N−H reductive deprotonation, two-electron N−H oxidative addition in primary amines was reported to be mediated by uranium[4] and phosphorus[6a] centers. In sharp contrast to the reactive N−H bond, the C−N bond in primary amines is much more inert and difficult to cleave. The poor electrophilicity of the -NH_2 group renders the C−NH_2 bond a challenging target for transition metal-catalyzed oxidative addition[42] and reductive deamination,[43] both of which are two-electron processes. As a footnote to the challenge, the organic synthesis community currently must convert the -NH_2 into a better leaving group to conduct deamination, such as via isodiazene intermediates in a recent example,[44] or using a strong Lewis acid catalyst such as $B(C_6F_5)_3$ coupled with silanes as the reductant.[45] With regard to azobenzene, it is a classic substrate for both one-electron and two-electron reductions. Noticeably, a bimetallic two-electron oxidative addition of azobenzene was recently reported to be facilitated by a U(+3) ↔ U(+5) interconversion, which demonstrated the presence of a two-electron process in uranium chemistry.[46]

https://doi.org/10.1021/acs.inorgchem.4c02914
Inorg. Chem. 2024, 63, 15247−15258

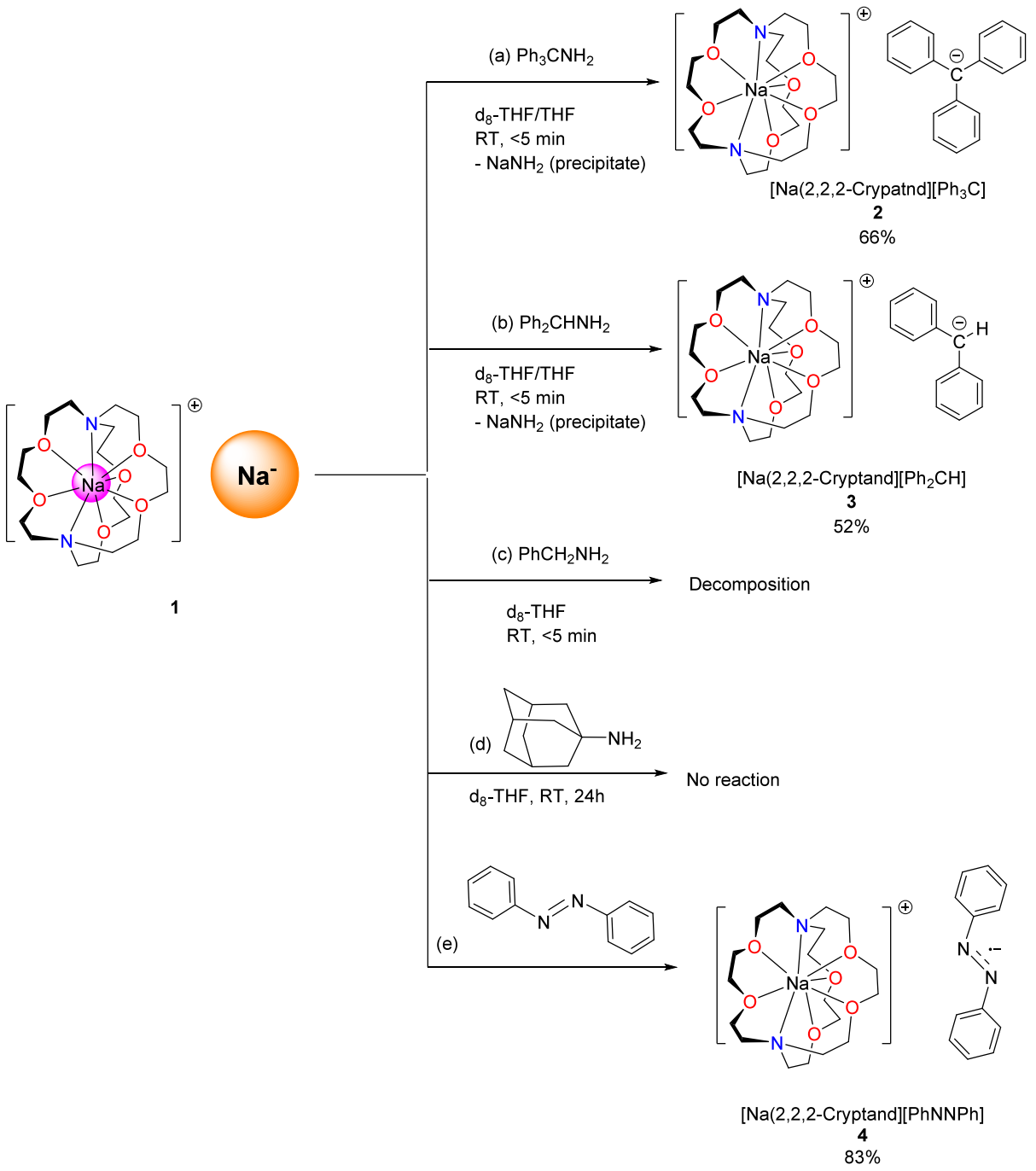

Figure 6. Overview of the reactivity of **1** toward (a) Ph_3CNH_2, (b) Ph_2CHNH_2, (c) $PhCH_2NH_2$, (d) adamantylamine, and (e) azobenzene.

The reaction between **1** and 1 equiv of trityl amine (Ph_3CNH_2) in d_8-THF (Figure 6a) resulted in an immediate color change from blue to red. ^{1}H NMR monitoring of the reaction mixture indicated the formation of a clean product. Scaling up the reaction in THF and crystallization led to the isolation of red crystals, the structure of which was unveiled by the SCXRD study to be $[Na(2,2,2\text{-cryptand})]^+[Ph_3C]^-$ separated ion pair (SIP) complex **2** (Figure 6a). The SCXRD structure of **2** is shown in Figure S23. In the Ph_3C^- anion, the central carbon atom features a distorted trigonal planar geometry with three $C^{cent}-C^{ipso}$ bonds with lengths of 1.44−1.47 Å. These structural parameters match those of the reported alkali metal trityl complexes.[47,48]

Given the challenging nature of primary amines' C−N bond cleavage,[41,42] the formation of **2** in high yield and under mild conditions is impressive. We rationalize **2** as the result of a two-electron oxidative addition of the Na^- center to the C−N bond in trityl amine, followed by the formation of $NaNH_2$ and **2** (Figure 7a). The formation of $NaNH_2$ could function as a thermodynamic driving force for the reaction. We did not observe any products from the potential one-electron reductive deprotonation, e.g., H_2 or Na(0) species, or the two-electron oxidative addition toward the N−H bond. Hence, in the case of trityl amine, the Na^- center in **1** exhibits highly selective single-metal two-electron C−N bond cleavage and deamination. Thermodynamic calculations were conducted to understand the driving force of the selectivity (Figure 7b),

https://doi.org/10.1021/acs.inorgchem.4c02914
Inorg. Chem. 2024, 63, 15247−15258

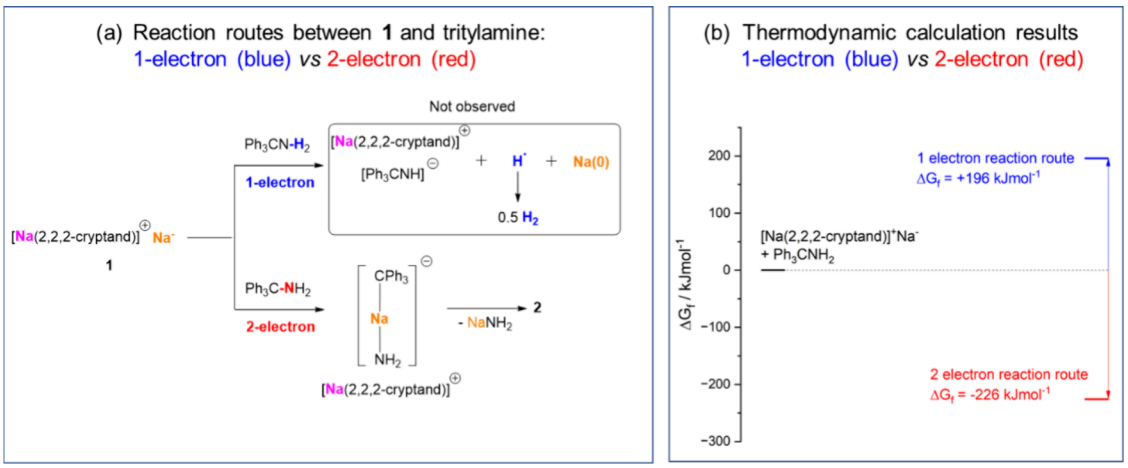

Figure 7. (a) Two possible reaction routes between **1** and trityl amine: one-electron reductive deprotonation vs two-electron oxidative addition/deamination (color codes indicate the different origins of Na in **1**, pink for Na^+ and yellow for Na^-). (b) Thermodynamic calculations for the two routes.

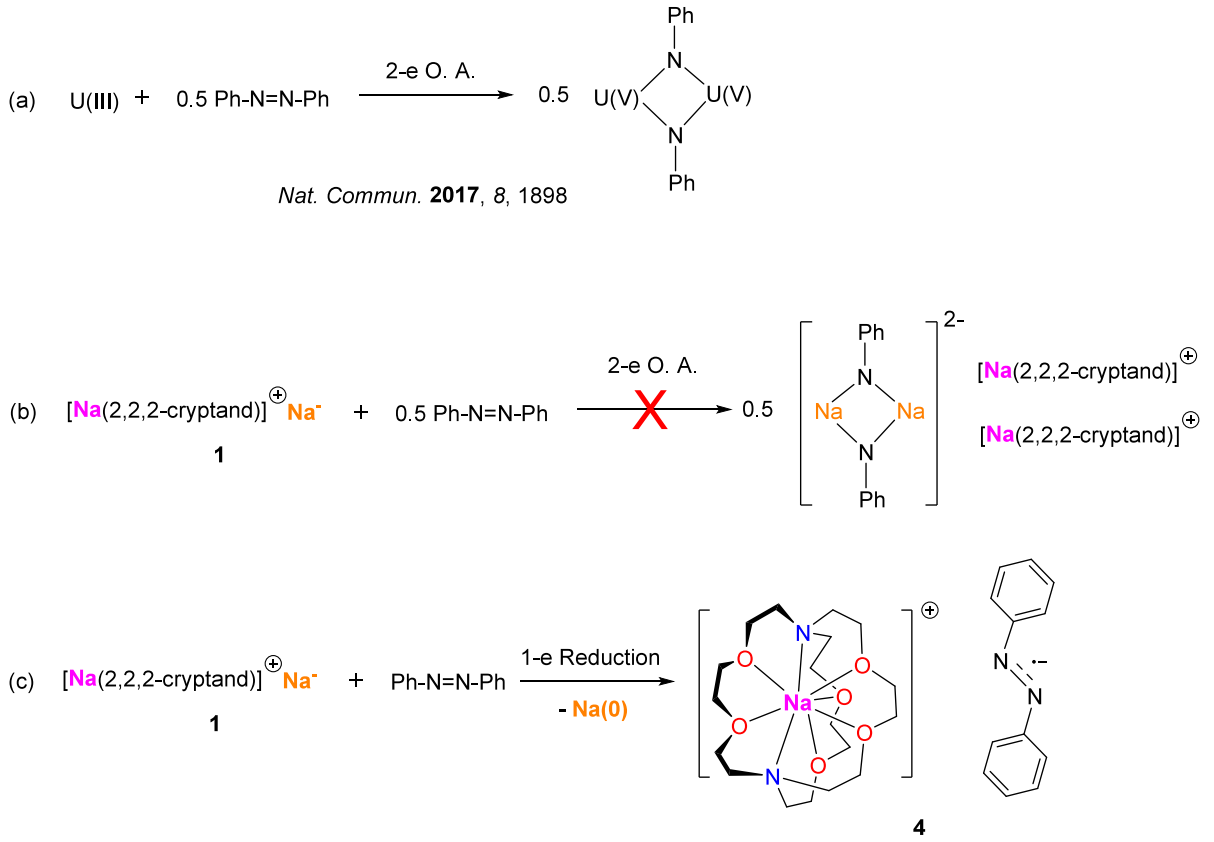

Figure 8. (a) Uranium-mediated two-electron oxidative addition toward azobenzene.[44] (b) Hypothetical two-electron oxidative addition between **1** and azobenzene, mimicking the uranium pattern, which was not observed herein. (c) What actually happened: one-electron reduction of azobenzene to produce SIP complex **3**, featuring an azobenzene radical monoanion.

with computational details given in Section 2 of the Supporting Information. The two-electron process was found to be exergonic, whereas the one-electron process was found to be endergonic; the differences in their Gibbs free energies of formation (ΔG_f) were calculated to be −226 kJ/mol (two-electron) and 196 kJ/mol (one-electron). While this approach neglects a variety of different important factors such as kinetics and the entropic gains as a result of the evolution of a gaseous product (for the hypothetical one-electron reductive deprotonation), the exer/endergonic nature of the two reactions qualitatively agrees with the experimental findings, suggesting that the two-electron route is more thermodynamically favorable.

It is noteworthy that, despite the fact that the trityl group is a widely used protective group for amines,[49] direct trityl amine deamination is scarce and requires a large excess of alkali metal on silica gel,[50] or iodine (I_2) to activate the -NH_2.[51] Similar to that of the trityl amine, the reaction between **1** and diphenylmethyl amine (Ph_2CHNH_2) produces corresponding deamination product [Na(2,2,2-cryptand)][Ph_2CH] (**3**) (Fig-

https://doi.org/10.1021/acs.inorgchem.4c02914
Inorg. Chem. 2024, 63, 15247−15258

ure 6b). The SCXRD structure of **3** is shown in Figure S24. It is noteworthy that some pale-colored precipitate was observed in both reactions to form **2** and **3**, which we postulated to be the $NaNH_2$ byproduct. It is well-known that $NaNH_2$ is insoluble in most hydrocarbon and ethereal solvents. Further reducing the steric bulkiness of the primary amine to benzyl amine ($PhCH_2NH_2$) leads to a fast reaction but decomposition (Figure 6c). We hypothesize that putative benzyl sodium SIP complex [Na(2,2,2-cryptand)][$PhCH_2$] (which is unknown to the best of our knowledge[52]) is unstable and induces decomposition.

Interestingly, in sharp contrast with the fast reactions between **1** and Ph_3CNH_2, Ph_2CHNH_2, or $PhCH_2NH_2$, **1** does not react with 1-adamantylamine (Figure 6d) even after several hours at room temperature. There are two possible reasons for the inertness of 1-adamantylamine. (1) The adamantyl group[53] is not as easy to reduce to the corresponding carbon anion as trityl or diphenylmethyl.[54] (2) The steric rigidity of the adamantyl group is less favorable for the two-electron oxidative addition intermediate. It is also noteworthy that one-electron reductive deprotonation was not observed in any of the three primary amines tested; i.e., the N−H bond did not react.

It is now obvious that in the cases of primary amines, **1** prefers the two-electron process over the one-electron process. Nevertheless, the scenario is different for azobenzene. We tested the reaction between **1** and 0.5 equiv of azobenzene (Figure 8b), aiming to mimic the reported U(+3) ↔ U(+5) two-electron oxidative addition (Figure 8a).[44] However, ^{1}H and ^{23}Na NMR monitoring of the reaction in d_8-THF indicates the presence of unreacted **1**, along with new broad ^{1}H NMR signals, which could be a new paramagnetic product(s). Hence, we increased the amount of azobenzene and increased the stoichiometric ratio to 1:1 (Figure 8c). Immediately after mixing at room temperature, the 1:1 reaction in d_8-THF produced a black/purple solution with a significant amount of gray/black fine solid precipitate, where the *in situ* ^{1}H and ^{23}Na NMR spectra indicate the full consumption of both of the starting materials, and exhibited a Na^+ ^{23}Na signal and a ^{1}H NMR spectrum with featureless and wide signals. Scaling up the 1:1 reaction in THF and recrystallization from a THF/hexane mixture under −35 °C produced purple crystals, which were confirmed by SCXRD to be an azobenzene radical monoanion SIP complex [Na(2,2,2-cryptand)][PhNNPh] (**4**) (Figures 6e and 8c). The SCXRD structure of **4** is shown in Figure S25, where the bond lengths and angles in the azobenzene radical monoanion match with the reported precedents.[55] The ^{1}H NMR spectrum of **4** is featureless in the aromatic region, which corroborates its radical nature, as reflected in the X-band solution EPR study (Figure S21). The radical property is further consolidated by computational studies (*vide infra*).

We conducted a DFT molecular orbital analysis of **4**. The singly occupied molecular orbital (SOMO) is delocalized across the $[PhNNPh]^{\bullet-}$ radical anion. In corresponding with the delocalized SOMO, spin density analysis indicated that the spin density is delocalized, as well. Such spin density delocalization has been widely reported in main-group radical complexes.[56] For the MO and spin density analyses of **4**, see the Supporting Information. We postulate that the Na(0) species, as the byproduct of the one-electron reduction, precipitate out as the gray/black solid and hence cannot be observed in the *in situ* solution-state ^{23}Na NMR spectrum in d_8-THF.

CONCLUSION

In conclusion, in this work, the first facile synthesis of sodide **1** allowed us to study systematically the sodide reactivity for the first time. We realized the first group 1 single-metal two-electron reduction in a challenging transformation, primary amine deamination. The two-electron versus one-electron reactivity of **1** is dependent on the substrate. **1** exhibits one-electron reduction toward azobenzene. Further work is underway in our group in two directions: (1) expanding the easy-access alkalide scope and (2) exploring the alkalides' potential in inert small molecule and chemical bond activations, particularly focusing on exploiting the new AM(−1) ↔ AM(+1) redox couple to mimic two-electron transition metal catalysis.

EXPERIMENTAL SECTION

General Procedures. All manipulations were carried out in a Vigor glovebox equipped with a −35 °C freezer and a cold well, under an atmosphere of dry argon. Solvents were dried with sodium press, a sodium−potassium alloy, distilled under reduced pressure, and kept in the glovebox. Chemicals were purchased from Merck, Fluorochem, or Alfa Aesar and dried under dynamic vacuum for several hours (for solids) or with activated 4 Å molecular sieves that had been frozen, thawed, and vacuum degassed (for liquid) prior to use. All glassware, including pipettes, vials, and ampules, was silylated by being treated with trimethylsilyl chloride (Me_3SiCl), rinsed with water, and dried in a 150 °C oven for 12 h prior to use.

Mechanochemical ball milling reactions were conducted using a Retsch MM400 mixer mill within a 25 mL Retsch stainless steel jar and a 10 mm diameter stainless steel ball (one ball per jar). For the *in situ* visual monitoring study, a 20 mm diameter three-dimensionally printed PMMA jar was used, which was sealed with electric tape in the glovebox.

Solution-state ^{1}H, ^{23}Na, and ^{13}C{^{1}H} NMR spectra were recorded on a Bruker 400 Avance III spectrometer or a Bruker 500 Avance III HD spectrometer operating at 400 or 500 MHz, respectively, for ^{1}H NMR, 132 or 106 MHz, respectively, for ^{23}Na NMR, and 101 or 126 MHz, respectively, for ^{13}C{^{1}H} NMR. Solid-state MAS ^{23}Na NMR was recorded on a Bruker 500 Avance III HD NMR spectrometer, operating at 132 MHz, with 4 mm rotors and a MAS rate of 10 kHz. Chemical shifts are quoted in parts per million and are relative to $SiMe_4$ (^{1}H and ^{13}C{^{1}H}) or external 0.1 M NaCl in D_2O (solution-state ^{23}Na) or external solid NaCl (solid-state MAS ^{23}Na).

Continuous-wave (CW) electron paramagnetic resonance (EPR) spectra were recorded on a Bruker EMX EPR spectrometer operating at the X-band frequency (9.4 GHz).

Synthesis and Characterization of [Na$^+$(2,2,2-cryptand)Na$^-$] (1). On a 1 mmol scale, [2.2.2]cryptand (0.3765 g, 1 mmol) and sodium metal (0.0460 g, 2 mmol) were combined in a 25 mL ball milling jar, with a 10 mm stainless steel ball. The jar was sealed in an argon glovebox. The mixture was ball milled on a Retch MM400 ball mill at 30 Hz for 10 min. During ball milling, the jar turned slightly warm. The jars were opened in the glovebox. A bronze powder resulted.

For the SCXRD study, the bronze powder was dissolved in THF (12 mL), and the resulting deep blue solution was filtered and placed in a −35 °C freezer. After 24 h, gold crystals suitable for SCXRD resulted. The mother liquor was removed, and the volatiles were removed *in vacuo*. A gold crystalline powder resulted (0.1612 g, 38% yield).

On a 2 mmol scale, [2.2.2]cryptand (0.7530 g, 2 mmol) and sodium metal (0.0920 g, 4 mmol) were combined in a 25 mL ball milling jar, with a 10 mm stainless steel ball. The jar was sealed in an argon glovebox. The mixture was ball milled on a Retch MM400 ball

https://doi.org/10.1021/acs.inorgchem.4c02914
Inorg. Chem. 2024, 63, 15247−15258

mill at 30 Hz for 10 min. During ball milling, the jar turned slightly warm. The jars were opened in the glovebox. A bronze powder resulted.

For crystallization, the bronze powder was dissolved in THF (10 mL), and the resulting deep blue solution was filtered and placed in a −35 °C freezer. After 24 h, gold crystals resulted. The mother liquor was removed, and the volatiles were removed *in vacuo*. A gold crystalline powder resulted (0.4023 g, 48% yield): ^{1}H NMR (500 MHz, d_8-THF, 25 °C) δ 3.63 (s, br, 12H, CH_2), 3.58 (s, br, 12H, CH_2), 2.64 (s, br, 12H, CH_2); ^{23}Na NMR (106 MHz, d_8-THF, 25 °C) δ 1132.2 (Na^0), −11.0 (Na^+), −62.1 (Na^-); ^{23}Na NMR (132 MHz, MAS solid-state, 25 °C) δ −10.3 (Na^+), −61.1 (Na^-).

Reactivity of [Na^+(2,2,2-cryptand)Na^-] (1). *Reaction of [Na^+(2,2,2-cryptand)Na^-] (1) with Triphenylmethylamine to Produce 2.* On a NMR scale, **1** (0.0169 g, 0.04 mmol) was dissolved in d_8-THF (0.25 mL). The resulting dark blue solution was added in one portion to a colorless solution of triphenylmethylamine (0.0104 g, 0.04 mmol) in d_8-THF (0.25 mL) that had been cooled in a −35 °C freezer. A deep red solution resulted. The solution was transferred to a J. Young NMR tube, and the reaction was monitored by ^{1}H and ^{23}Na NMR.

For scaling up, **1** (0.1098 g, 0.26 mmol) was dissolved in THF (1.5 mL). The resulting dark blue solution was added in one portion to a colorless solution of triphenylmethylamine (0.0674 g, 0.26 mmol) in THF (1 mL) that had been cooled in a −35 °C freezer. A deep red solution resulted. The solution was left at room temperature for 45 min, before being filtered. *n*-Hexane (0.5 mL) was added, and the solution was placed in a −35 °C freezer. Crystals suitable for SCXRD resulted after 30 min. The mother liquor was removed, and the crystals were washed with *n*-hexane (2 mL) and dried *in vacuo*. Red crystals resulted (0.1100 g, 66% yield): ^{1}H NMR (400 MHz, d_8-THF, 25 °C) δ 7.29 (d, J = 8.2 Hz, ArH, 6H), 6.50 (t, J = 7.7 Hz, ArH, 6H), 5.97−5.88 (m, ArH, 3H), 3.54 (s, CH_2, 12H), 3.52−3.47 (m, CH_2, 12H), 2.61−2.54 (m, CH_2, 12H); ^{23}Na NMR (106 MHz, d_8-THF, 25 °C) δ −11.1 (Na^+); ^{13}C{^{1}H} NMR (101 MHz, d_8-THF, 25 °C) δ 150.1, 128.1, 124.4, 112.9, 69.4, 68.5, 53.8.

Reaction of [Na^+(2,2,2-cryptand)Na^-] (1) with Benzhydrylamine to Produce 3. On a NMR scale, **1** (0.0169 g, 0.04 mmol) was dissolved in d_8-THF (0.25 mL). The resulting dark blue solution was added in one portion to a colorless solution of benzhydrylamine (0.0073 g, 0.04 mmol) in d_8-THF (0.25 mL) that had been cooled in a −35 °C freezer. A dark red/orange cloudy solution resulted. The solution was transferred to a J. Young NMR tube, and the reaction was monitored by ^{1}H and ^{23}Na NMR.

For scaling up, **1** (0.1056 g, 0.25 mmol) was dissolved in THF (1.5 mL). The resulting dark blue solution was added in one portion to a colorless solution of benzhydrylamine (0.0458 g, 0.25 mmol) in THF (1.5 mL) that had been cooled in a −35 °C freezer. A deep red/orange cloudy solution resulted. The solution was left at room temperature for 30 min, before being filtered twice, and the solution was placed in a −35 °C freezer. Crystals suitable for SCXRD resulted overnight. The mother liquor was removed, and the crystals were washed with *n*-hexane (2 × 1 mL) and dried *in vacuo*. Red crystals resulted (0.0738 g, 52% yield): ^{1}H NMR (400 MHz, d_8-THF, 25 °C) δ 6.66−6.25 (m, ArH, 8H), 5.61−5.46 (m, ArH, 2H), 4.32 (s, CH, 1H), 3.44 (s, CH_2, 12H), 3.41 (t, J = 5.0 Hz, CH_2, 12H), 2.47 (t, J = 4.8 Hz, CH_2, 12H); ^{23}Na NMR (106 MHz, d_8-THF, 25 °C) δ −10.8 (Na^+); ^{13}C{^{1}H} NMR (101 MHz, d_8-THF, 25 °C) δ 147.1, 128.1, 106.0, 82.0, 69.3, 68.5, 53.8.

Reaction of [Na^+(2,2,2-cryptand)Na^-] (1) with Benzylamine. On a NMR scale, **1** (0.0169 g, 0.04 mmol) was dissolved in d_8-THF (0.25 mL). The resulting dark blue solution was added in one portion to a colorless solution of benzylamine (0.0043 g, 0.04 mmol) in d_8-THF (0.25 mL) that had been cooled in a −35 °C freezer. A dark blue solution resulted, which was transferred to a J. Young NMR tube. Within 5 min, the solution turned into a cloudy pale blue/gray mixture with insolubles, which is suspected to be due to fast decomposition of the reaction product. ^{1}H and ^{23}Na NMR was recorded (Figures S17 and S18).

Reaction of [Na^+(2,2,2-cryptand)Na^-] (1) with Azobenzene to Produce 4. On a NMR scale, **1** (0.0169 g, 0.04 mmol) was dissolved in d_8-THF (0.25 mL). The resulting dark blue solution was added in one portion to a colorless solution of azobenzene (0.0073 g, 0.04 mmol) in d_8-THF (0.25 mL) that had been cooled in a −35 °C freezer. A cloudy dark red/brown solution resulted. The solution was transferred to a J. Young NMR tube, and the reaction was monitored by ^{1}H and ^{23}Na NMR.

For scaling up, **1** (0.0670 g, 0.16 mmol) was dissolved in THF (1.5 mL). The resulting dark blue solution was added in one portion to an orange solution of azobenzene (0.0292 g, 0.16 mmol) in THF (1.5 mL) that had been cooled in a −35 °C freezer. A brown cloudy solution resulted. The solution was left at room temperature for 30 min before the volatiles were removed *in vacuo*, and the crystalline solid was washed with *n*-hexane (2 × 2 mL) and dried *in vacuo* (0.0770 g, 83% yield).

Purple crystals suitable for SCXRD resulted after 6 h from a THF (5 mL) solution that was filtered, followed by the addition of *n*-hexane (1 mL), and placed in a −35 °C freezer: ^{1}H NMR (400 MHz, d_8-THF, 25 °C) δ 3.35 (s, br, CH_2, 24H), 2.47 (s, br, CH_2, 12H) (the [PhNNPh]$^{\bullet-}$ fragment is NMR silent); ^{23}Na NMR (106 MHz, d_8-THF, 25 °C) δ −10.5 (Na^+).

Attempted Reaction of [Na^+(2,2,2-cryptand)Na^-] (1) with 1-Adamantylamine. On a NMR scale, **1** (0.0169 g, 0.04 mmol) was dissolved in d_8-THF (0.5 mL). The resulting dark blue solution was added in one portion to a colorless solution of 1-adamantylamine (0.0061 g, 0.04 mmol) in d_8-THF (0.5 mL) that had been cooled in a −35 °C freezer. No observable color change resulted. The solution was transferred to a J. Young NMR tube, and the reaction was monitored by ^{1}H and ^{23}Na NMR, which showed no reaction between **1** and 1-adamantylamine and decomposition of **1** within 1 day.

■ ASSOCIATED CONTENT

Supporting Information

The Supporting Information is available free of charge at https://pubs.acs.org/doi/10.1021/acs.inorgchem.4c02914.

Additional experimental details, materials, and methods, including photographs of the experimental setup (PDF)

Accession Codes

CCDC 2336129, 2351275, 2351363, and 2355684 contain the supplementary crystallographic data for this paper. These data can be obtained free of charge via www.ccdc.cam.ac.uk/data_request/cif, or by emailing data_request@ccdc.cam.ac.uk, or by contacting The Cambridge Crystallographic Data Centre, 12 Union Road, Cambridge CB2 1EZ, UK; fax: +44 1223 336033.

■ AUTHOR INFORMATION

Corresponding Authors

Erli Lu − *School of Chemistry, University of Birmingham, Birmingham B15 2TT, U.K.; Chemistry, School of Natural and Environmental Sciences, Newcastle University, Newcastle upon Tyne NE1 7RU, U.K.;* orcid.org/0000-0002-0619-5967; Email: e.lu@bham.ac.uk

Jack M. Hemingway − *Chemistry, School of Natural and Environmental Sciences, Newcastle University, Newcastle upon Tyne NE1 7RU, U.K.*; Email: jack.hemingway@newcastle.ac.uk

Paul G. Waddell − *Chemistry, School of Natural and Environmental Sciences, Newcastle University, Newcastle upon Tyne NE1 7RU, U.K.*; Email: paul.waddell@newcastle.ac.uk

Corinne Wills − *Chemistry, School of Natural and Environmental Sciences, Newcastle University, Newcastle*

upon Tyne NE1 7RU, U.K.; Email: corinne.wills@newcastle.ac.uk

Authors

Nathan Davison − *School of Chemistry, University of Birmingham, Birmingham B15 2TT, U.K.; Chemistry, School of Natural and Environmental Sciences, Newcastle University, Newcastle upon Tyne NE1 7RU, U.K.*

Tomislav Stolar − *Federal Institute for Materials Research and Testing (BAM), 12489 Berlin, Germany;* orcid.org/0000-0002-9824-4462

Casey M. Dixon − *Chemistry, School of Natural and Environmental Sciences, Newcastle University, Newcastle upon Tyne NE1 7RU, U.K.*

Luke Barron − *Chemistry, School of Natural and Environmental Sciences, Newcastle University, Newcastle upon Tyne NE1 7RU, U.K.*

James A. Dawson − *Chemistry, School of Natural and Environmental Sciences, Newcastle University, Newcastle upon Tyne NE1 7RU, U.K.;* orcid.org/0000-0002-3946-5337

Complete contact information is available at: https://pubs.acs.org/10.1021/acs.inorgchem.4c02914

Funding

E.L. and J.A.D. thank the Newcastle University Academic Track Fellowship scheme. N.D., J.M.H., J.A.D., and E.L. thank the Leverhulme Trust for generous financial support via Research Grants RPG-2022-231 and RPG-2023-159.

Notes

The authors declare no competing financial interest.

■ ACKNOWLEDGMENTS

The authors thank the Newcastle University Chemistry Technical Support Team (Dr. Amy Roberts and Mr. Niall Straughan) for supporting our research.

■ DEDICATION

This paper is in memory of Professor Li-Xin Dai, Shanghai Institute of Organic Chemistry, who sadly passed away on May 13, 2024 (1924−2024).

■ REFERENCES

(1) Labinger, J. A. Tutorial on Oxidative Addition. *Organometallics* **2015**, *34*, 4784−4795.

(2) For a very recent example, see: Wang, Y.; Liang, J.; Deng, C.; Sun, R.; Fu, P.-X.; Wang, B.-W.; Gao, S.; Huang, W. Two-Electron Oxidation at a Single Cerium Center. *J. Am. Chem. Soc.* **2023**, *145*, 22466−22474.

(3) For a review, see: Lu, E.; Liddle, S. T. Uranium-mediated oxidative addition and reductive elimination. *Dalton Trans.* **2015**, *44*, 12924−12941.

(4) For a very recent example, see: Fang, W.; Li, Y.; Zhang, T.; Rajeshkumar, T.; del Rosal, I.; Zhao, Y.; Wang, T.; Wang, S.; Maron, L.; Zhu, C. Oxidative Addition of E-H (E = C, N) Bonds to Transient Uranium(II) Centers. *Angew. Chem., Int. Ed.* **2024**, No. e202407339.

(5) For reviews, see: (a) Chu, T.; Nikonov, G. I. Oxidative Addition and Reductive Elimination at Main-Group Element Centers. *Chem. Rev.* **2018**, *118*, 3608−3680. (b) Weetman, C.; Inoue, S. The Road Travelled: After Main-Group Elements as Transition Metals. *ChemCatChem.* **2018**, *10*, 4213−4228. (c) Parr, J. M.; Crimmin, M. R. Carbon-carbon bond activation by Mg, Al, and Zn complexes. *Chem. Sci.* **2023**, *14*, 11012−11021.

(6) (a) Zhao, W.; McCarthy, S. M.; Lai, T. Y.; Yennawar, H. P.; Radosevich, A. T. Reversible Intermolecular E-H Oxidative Addition to a Geometrically Deformed and Structurally Dynamic Phosphorous Triamide. *J. Am. Chem. Soc.* **2014**, *136*, 17634−17644. (b) Biskup, D.; Schnakenburg, G.; Boeré, R. T.; Espinosa Ferao, A.; Streubel, R. K. Challenging an old paradigm by demonstrating transition metal-like chemistry at a neutral nonmetal center. *Nat. Commun.* **2023**, *14*, 6456.

(7) (a) Dye, J. L. Compounds of Alkali Metal Anions. *Angew. Chem., Int. Ed.* **1979**, *18*, 587−598. (b) Dye, J. L. The alkali metals: 200 years of surprises. *Philos. Trans. R. Soc.* **2015**, *A373*, 20140174.

(8) Dye, J. L.; Ceraso, J. M.; Lok, M. T.; Barnett, B. L.; Tehan, F. J. A Crystalline Salt of the Sodium Anion (Na^-). *J. Am. Chem. Soc.* **1974**, *96*, 608−609.

(9) Tehan, F. J.; Barnett, B. L.; Dye, J. L. Alkali Anions. Preparation and Crystal Structure of a Compound Which Contains the Cryptated Sodium Cation and the Sodium Anion. *J. Am. Chem. Soc.* **1974**, *96*, 7203−7208.

(10) For instances, see: (a) Chapter 3-4: Alkalides and Electrides. In *Advanced Inorganic Chemistry*, 6th ed.; Cotton, F. A., Wilkinson, G., Murillo, C. A., Bochmann, M., Eds.; John Wiley & Sons, Inc., 1999. (b) The Alkali Metal Group. In *Inorganic Chemistry*; Holleman, A. F., Wiberg, E., Eds.; Academic Press: San Diego, 2001; p 1085.

(11) Dye, J. L. Alkali Metal Anions. An unusual oxidation state. *J. Chem. Educ.* **1977**, *54*, 332−339.

(12) Dye, J. L. Anions of the Alkali Metals. *Sci. Am.* **1977**, *237*, 92−105.

(13) Dale, S. G.; Johnson, E. R. Thermodynamic cycles of the alkali metal-ligand complexes central to electride formation. *Phys. Chem. Chem. Phys.* **2017**, *19*, 12816−12825.

(14) Chaban, V. V.; Prezhdo, O. V. Electron Solvation in Liquid Ammonia: Lithium, Sodium, Magnesium, and Calcium as Electron Sources. *J. Phys. Chem. B* **2016**, *120*, 2500−2506.

(15) Ariyarathna, I. R. Ground and excited electronic structures of electride and alkalide units: The cases of Metal-Tren, -Azacryptand, and -TriPip222 complexes. *J. Comput. Chem.* **2023**, DOI: 10.1002/jcc.27265.

(16) Seel, A. G.; Holzmann, N.; Imberti, S.; Bernasconi, L.; Edwards, P. P.; Cullen, P. L.; Howard, C. A.; Skipper, N. T. Solvation of Na^- in the Sodide Solution, $LiNa{\cdot}10MeNH_2$. *J. Phys. Chem. B* **2019**, *123*, 5337−5342.

(17) (a) Grobelny, Z.; Stolarzewicz, A.; Morejko-Buz, B.; Maercker, A.; Krompiec, S.; Bieg, T. Regioselectivity of the ring opening in the reaction of phenyloxirane, (phenylmethyl)oxirane and (2-phenylethyl)oxirane with K^-, $K^+(15\text{-crown-}5)_2$. *J. Organomet. Chem.* **2003**, *672*, 43−51. (b) Grobelny, Z. The behaviour of organopotassium intermediates derived from oxiranes under the influence of alkalide K^-, $K^+(15\text{-crown-}5)_2$. *J. Organomet. Chem.* **2003**, *677*, 118−124. (c) Grobelny, Z.; Stolarzewicz, A.; Maercker, A.; Krompiec, S.; Kasperczyk, J.; Rzepa, J. Decomposition of vinyl ethers by alkalide K^-, $K^+(15\text{-crown-}5)_2$ via organopotassium intermediates. *J. Organomet. Chem.* **2004**, *689*, 1580−1585. (d) Grobelny, Z.; Stolarzewicz, A.; Maercker, A.; Krompiec, S.; Kasperczyk, J.; Rzepa, J.; Frey, H. Electron-transfer reduction of selected alcohols with alkalide K^-, $K^+(15\text{-crown-}5)_2$ via organometallic intermediates. *J. Organomet. Chem.* **2004**, *689*, 2361−2367.

(18) Cauliez, P. M.; Jackson, J. E.; Dye, J. L. An unusual reduction of ethylene occurring during the thermal decomposition of alkalides and electrides. *Tetrahedron Lett.* **1991**, *32*, 5039−5042.

(19) Ichimura, A. S.; Huang, R. H.; Xie, Q.; Morganelli, P.; Burns, A.; Dye, J. L. One-Dimensional Zigzag Chains of Cs^-: The Structures and Properties of $Li^+(Cryptand[2.1.1])Cs^-$ and $Cs^+(Cryptand[2.2.2])Cs^-$. *J. Phys. Chem. B* **2006**, *110*, 12293−12301.

(20) Dye, J. L. Preparation and Analysis of Metal/Solvent Solutions and the Formation of Alkali Metal Anions. *J. Phys. Chem.* **1980**, *84*, 1084−1090.

(21) Le, L. D.; Issa, D.; van Eck, B.; Dye, J. L. Preparation of Alkalide and Electride Films by Direct Vapor Deposition. *J. Phys. Chem.* **1982**, *86*, 7−9.

(22) (a) Kim, J.; Ichimura, A. S.; Huang, R. H.; Redko, M. Y.; Phillips, R. C.; Jackson, J. E.; Dye, J. L. Crystalline Salts of Na^- and K^- (Alkalides) that Are Stable at Room Temperature. *J. Am. Chem. Soc.* **1999**, *121*, 10666−10667. (b) Redko, M. Y.; Vlassa, M.; Jackson, J. E.; Misiolek, A. W.; Huang, R. H.; Dye, J. L. "Inverse Sodium Hydride": A Crystalline Salt that Contains H+ and Na^-. *J. Am. Chem. Soc.* **2002**, *124*, 5928−5929. (c) Redko, M. Y.; Huang, R. H.; Jackson, J. E.; Harrison, J. F.; Dye, J. L. Barium Azacryptand Sodide, the First Alkalide with an Alkaline Earth Cation, Also Contains a Novel Dimer, $(Na_2)2^-$. *J. Am. Chem. Soc.* **2003**, *125*, 2259−2263. (d) Redko, M. Y.; Jackson, J. E.; Huang, R. H.; Dye, J. L. Design and Synthesis of a Thermally Stable Organic Electride. *J. Am. Chem. Soc.* **2005**, *127*, 12416−12422.

(23) Grobelny, Z.; Stolarzewicz, A.; Sokol, M.; Grobelny, J.; Janeczek, H. Enhanced Stability of Potassium Solutions in Tetrahydrofuran Containing 15-Crown-5. *J. Phys. Chem.* **1992**, *96*, 5193−5196.

(24) Mechanochemistry is emerging to provide versatile and sustainable synthetic tools. For a selection of Reviews from 2023 and 2024, see: (a) Ardila-Fierro, K. J.; Hernández, J. G. Intermediates in Mechanochemical Reactions. *Angew. Chem., Int. Ed.* **2024**, *63*, No. e202317638. (b) Wenger, L. E.; Hanusa, T. P. Synthesis without solvent: consequences for mechanochemical reactivity. *Chem. Commun.* **2023**, *59*, 14210−14222. (c) Lee, J. S.; Han, G.-F.; Baek, J.-B. Mechanochemical Ammonia Synthesis: Old is New Again. *ChemSusChem* **2023**, *16*, No. e202300459. (d) Naidu, B. R.; Sruthi, T.; Mitty, R.; Venkateswarlu, K. Catalyst-free mechanochemistry as a versatile tool in synthetic chemistry: a review. *Green Chem.* **2023**, *25*, 6120−6148. (e) Reynes, J. F.; Isoni, V.; García, F. Tinkering with Mechanochemical Tools for Scale Up. *Angew. Chem., Int. Ed.* **2023**, *62*, No. e202300819. (f) Auvray, T.; Friščić, T. Shaking Things from the Ground-Up: A Systematic Overview of the Mechanochemistry of Hard and High-Melting Inorganic Materials. *Molecules* **2023**, *28*, 897. (g) Martinez, V.; Stolar, T.; Karadeniz, B.; Brekalo, I.; Užarević, K. Advancing mechanochemical synthesis by combining milling with different energy sources. *Nat. Rev. Chem.* **2023**, *7*, 51−65.

(25) As a new trend, mechanochemistry ball milling has recently been introduced into s-block metal chemistry: (a) Jędrzkiewicz, D.; Mai, J.; Langer, J.; Mathe, Z.; Patel, N.; DeBeer, S.; Harder, S. Access to a Labile Monomeric Magnesium Radical by Ball-Milling. *Angew. Chem., Int. Ed.* **2022**, *61*, No. e202200511. (b) Jędrzkiewicz, D.; Langer, J.; Harder, S. Low-valent Mg(I) complexes by ball-milling. *Z. Anorg. Allg. Chem.* **2022**, *648*, No. e202200138. (c) Gao, Y. P.; Kubota, K.; Ito, H. Mechanochemical Approach for Air-Tolerant and Extremely Fast Lithium-Based Birch Reductions in Minutes. *Angew. Chem., Int. Ed.* **2023**, *62*, No. e202217723. (d) Davison, N.; Quirk, J. A.; Tuna, F.; Collison, D.; McMullin, C. L.; Michaels, H.; Morritt, G. H.; Waddell, P. G.; Gould, J. A.; Freitag, M.; Dawson, J. A.; Lu, E. A room-temperature stable electride and its reactivity: reductive benzene/pyridine couplings and solvent-free Birch reductions. *Chem* **2023**, *9*, 576−591. (e) Davison, N.; Khatun, T.; Arce-Garcia, I.; Gould, J. A.; Dawson, J. A.; Lu, E. Facile Mechanochemical Reduction and Lithium-Ion Doping of Transition-Metal Oxides. *Eur. J. Inorg. Chem.* **2023**, *26*, No. e202300344. (f) Davison, N.; Waddell, P. G.; Lu, E. Reduction of K^+ or Li^+ in the Heterobimetallic Electride $K^+[LiN(SiMe_3)_2]e^-$. *J. Am. Chem. Soc.* **2023**, *145*, 17007−17012. (g) Kondo, K.; Kubota, K.; Ito, H. Mechanochemistry enabling highly efficient Birch reduction using sodium lumps and d-(+)-glucose. *Chem. Sci.* **2024**, *15*, 4452.

(26) Gao, P.; Jiang, J.; Maeda, S.; Kubota, K.; Ito, H. Mechanochemically Generated Calcium-Based Heavy Grignard Reagents and Their Application to Carbon-Carbon Bond-Forming Reactions. *Angew. Chem., Int. Ed.* **2022**, *61*, No. e202207118.

(27) Kubota, K.; Fukuzawa, Y.; Kondo, K.; Gao, Y.; Ito, H. Highly efficient and air-tolerant calcium-based Birch reduction using mechanochemistry. *Chem. Lett.* **2024**, *53*, upae060.

(28) Nallaparaju, J. V.; Satsi, R.; Merzhyievskyi, D.; Jarg, T.; Aav, R.; Kananovich, D. G. Mechanochemical Birch Reduction with Low Reactive Alkaline Earth Metals. *Angew. Chem., Int. Ed.* **2024**, *63*, No. e202319449.

(29) Dye, J. L.; Andrews, C. W.; Ceraso, J. M. Nuclear Magnetic Resonance Studies of Alkali Metal Anions. *J. Phys. Chem.* **1975**, *79*, 3076−3079.

(30) Kim, J.; Dye, J. L. Single-Crystal ^{23}Na NMR Study of Na^+(cryptand [2.2.2])Na^-. *J. Phys. Chem.* **1990**, *94*, 5399−5402.

(31) (a) Dye, J. L.; Nicely, V. A. A General Purpose Curvefitting Program for Class and Research Use. *J. Chem. Educ.* **1971**, *48*, 443−448. (b) Boss, R. D.; Popov, A. I. A Competitive NMR Technique for Measurements of Metal Ion-Macrocyclic Polyether Complexation Constant in Solutions. *Inorg. Chem.* **1985**, *24*, 3660−3664.

(32) Riedel, R.; Seel, A. G.; Malko, D.; Miller, D. P.; Sperling, B. T.; Choi, H.; Headen, T. F.; Zurek, E.; Porch, A.; Kucernak, A.; Pyper, N. C.; Edwards, P. P.; Barrett, A. G. M. Superalkali-Alkalide Interactions and Ion Pairing in Low-Polarity Solvents. *J. Am. Chem. Soc.* **2021**, *143*, 3934−3943.

(33) (a) Ceraso, J. M.; Dye, J. L. ^{23}Na NMR spectrum of the sodium anion. *J. Chem. Phys.* **1974**, *61*, 1585−1587. (b) Edwards, P. P.; Guy, S. C.; Holton, D. M.; McFarlane, W. N.m.r. Spectrum of Na^- in Sodium-Hexamethylphosphoric Triamide Solutions. *J. Chem. Soc., Chem. Commun.* **1981**, 1185−1186. (c) Edwards, P. P.; Guy, S. C.; Holton, D. M.; Johnson, D. C.; Sienko, M. J.; McFarlane, W.; Wood, B. Nuclear Magnetic Resonance Spectrum of the Sodium Anion in Sodium-*N,N*-Diethylacetamide Solutions: The Sodide Ion in the Presence of a Carbonyl Moiety. *J. Phys. Chem.* **1983**, *87*, 4362−4363. (d) Edwards, P. P. Magnetic Resonace Studies of Alkali Metals in Nonaqueous Solvents. *J. Phys. Chem.* **1984**, *88*, 3772−3780. (e) Phillips, R. C.; Khazaeli, S.; Dye, J. L. Sodium-23 Nuclear Magnetic Resonance Study of Sodium Metal in Methylamine Solutions That Contain 18-Crown-6. Kinetics of Sodium Cation-Sodide Ion Exchange. *J. Phys. Chem.* **1985**, *89*, 606−612. (f) Holton, D. M.; Edwards, P. P.; Johnson, D. C.; Page, C. J.; McFarlane, W.; Wood, B. Multielement NMR and ESR Study of Solutions of the Alkali Metals Na to Cs in *N,N*-Diethylacetamide, *N,N*-Dipropylacetamide, *N,N*-Dimethylpropanamide, and Tetramethylurea. *J. Am. Chem. Soc.* **1985**, *107*, 6499−6504. (g) Pyper, N. C.; Edwards, P. P. Nuclear Shielding in the Alkali Metal Anions. *J. Am. Chem. Soc.* **1986**, *108*, 78−81.

(34) Kim, J.; Dye, J. L. Single-Crystal ^{23}Na NMR Study of Na^+(cryptand [2.2.2])Na^-. *J. Phys. Chem.* **1990**, *94*, 5399−5402.

(35) (a) Dye, J. L.; Nicely, V. A. A General Purpose Curvefitting Program for Class and Research Use. *J. Chem. Educ.* **1971**, *48*, 443−448. (b) Boss, R. D.; Popov, A. I. A Competitive NMR Technique for Measurements of Metal Ion-Macrocyclic Polyether Complexation Constant in Solutions. *Inorg. Chem.* **1985**, *24*, 3660−3664.

(36) Kaneko, M.; Suzaki, A.; Muraoka, A.; Gotoh, K.; Yamashita, K. Neural network to predict ^{23}Na NMR spectra of Na_n clusters. *J. Mater. Inf.* **2023**, *3*, 8.

(37) Bayley, P. M.; Trease, N. M.; Grey, C. P. Insights into Electrochemical Sodium Metal Deposition as Probed with *in Situ* ^{23}Na NMR. *J. Am. Chem. Soc.* **2016**, *138*, 1955−1961.

(38) Dye, J. L.; Lok, M. T.; Tehan, F. J.; Coolen, R. B.; Papadakis, N.; Ceraso, J. M.; Debacker, M. G. Alkali Metal solutions Effect of Two Cyclic Polyethers on solubility and Spectra. *Ber. Bunsenges. Phys. Chem.* **1971**, *75*, 659−662.

(39) Dale, S. G.; Johnson, E. R. Thermodynamic cycles of the alkali metal-ligand complexes central to electride formation. *Phys. Chem. Chem. Phys.* **2017**, *19*, 12816−12825.

(40) Facelli, J. C. Chemical shift tensors: Theory and application to molecular structural problems. *Prog. Nucl. Mag. Res. Spec.* **2011**, *58*, 176−201.

(41) Knüpfer, C.; Klerner, L.; Mai, J.; Langer, J.; Harder, S. s-Block metal complexes of superbulky $(^tBu_3Si)_2N^-$: a new weakly coordinating anion? *Chem. Sci.* **2024**, *15*, 4386−4395.

(42) (a) Ouyang, K.; Hao, W.; Zhang, W.-X.; Xi, Z.-F. Transition-Metal-Catalyzed Cleavage of C-N Single Bonds. *Chem. Rev.* **2015**, *115*, 12045−12090. (b) Wang, Q.-J.; Su, Y.-J.; Li, L.-X.; Huang, H.-M. Transition-metal catalysed C-N bond activation. *Chem. Soc. Rev.*

https://doi.org/10.1021/acs.inorgchem.4c02914
Inorg. Chem. 2024, 63, 15247−15258

2016, *45*, 1257−1272. (c) García -Cárceles, J.; Bahou, K. A.; Bower, J. F. Recent Methodologies That Exploit Oxidative Addition of C-N Bonds to Transition Metals. *ACS Catal.* **2020**, *10*, 12738−12759.
(43) Berger, K. J.; Levin, M. D. Reframing primary alkyl amines as aliphatic building blocks. *Org. Biomol. Chem.* **2021**, *19*, 11−36.
(44) Berger, K. J.; Driscoll, J. L.; Yuan, M.; Dherange, B. D.; Gutierrez, O.; Levin, M. D. Direct Deamination of Primary Amines via Isodiazene Intermediates. *J. Am. Chem. Soc.* **2021**, *143*, 17366−17373.
(45) Fang, H.; Oestreich, M. Reductive Deamination with Hydeosilanes Catalyzed by $B(C_6F_5)_3$. *Angew. Chem., Int. Ed.* **2020**, *59*, 11394−11398.
(46) Gardner, B. M.; Kefalidis, C. E.; Lu, E.; Patel, D.; McInnes, E. J. L.; Tuna, F.; Wooles, A. J.; Maron, L.; Liddle, S. T. Evidence for single metal two electron oxidative addition and reductive elimination at uranium. *Nat. Commun.* **2017**, *8*, 1898.
(47) Tomboulian, P. Chemistry of Trityllithium. Direct Preparation and Some Reactions. *J. Org. Chem.* **1959**, *24*, 229−234.
(48) Brooks, J. J.; Stucky, G. D. π Groups in Ion Pair Bonding. Triphenylmethyllithium Tetramethylethylenediamine. *J. Am. Chem. Soc.* **1972**, *94*, 7333−7338.
(49) Green, T. W.; Wuts, P. G. M. *Protective Groups in Organic Synthesis*; Wiley-Interscience: New York, 1999; Vol. *583*−*584*, pp 744−747.
(50) Nandi, P.; Dye, J. L.; Jackson, J. E. Reductive amine deallyl- and debenzylation with alkali metal in Silica Gel (M-SG). *Tetrahedron Lett.* **2009**, *50*, 3864−3866.
(51) Duan, Y.; Zhong, W.; Zeng, Z.; Feng, J.; Xu, J.; Yang, F.; Liu, J. Iodine-promoted transfer of dihydrogen from ketones to alkenes, triphenylmethyl, and diphenylmethyl derivatives. *Chem. Commun.* **2023**, *60*, 75−78.
(52) Davison, N.; Lu, E. The quest for organo-alkali metal monomers: unscrambling the structure-reactivity relationship. *Dalton Trans.* **2023**, *52*, 8172−8192.
(53) Kruppa, G. H.; Beauchamp, J. L. Energetics and structure of the 1- and 2-adamantyl radicals and their corresponding carbonium ions by photoelectron spectroscopy. *J. Am. Chem. Soc.* **1986**, *108*, 2162−2169.
(54) Tidwell, T. T. Chapter 1 Triarylmethyl and Related Radicals. In *Stable Radicals: Fundamentals and Applied Aspects of Odd-Electron Compounds*; Hicks, R. G., Ed.; John Wiley & Sons, Inc., 2010.
(55) Evans, W. J.; Drummond, D. K.; Chamberlain, L. R.; Doedens, R. J.; Bott, S. G.; Zhang, H.; Atwood, J. L. Synthetic, Structural, and Reactivity Studies of the Reduction and CO Derivatization of Azobenzene Mediated by Divalent Lanthanide Complexes. *J. Am. Chem. Soc.* **1988**, *110*, 4983−4994.
(56) Lichtenberg, C. Main-Group Metal Complexes in Selective Bond Formations Through Radical Pathways. *Chem. - Eur. J.* **2020**, *26*, 9674−9687.

https://doi.org/10.1021/acs.inorgchem.4c02914
Inorg. Chem. 2024, 63, 15247−15258